FEBS 27767

FEBS Letters 555 (2003) 45–50

Minireview

Proton transfer pathways and mechanism in bacterial reaction centers

M.L. Paddock, G. Feher, M.Y. Okamura*

Department of Physics 0319, University of California San Diego, La Jolla, CA 92093, USA

Received 25 August 2003; accepted 1 September 2003

First published online 20 October 2003

Edited by Gunnar von Heijne, Jan Rydström and Peter Brzezinski

Abstract **The focus of this minireview is to discuss the state of knowledge of the pathways and rates of proton transfer in the bacterial reaction center (RC) from *Rhodobacter sphaeroides*. Protons involved in the light driven catalytic reduction of a quinone molecule Q_B to quinol Q_BH_2 travel from the aqueous solution through well defined proton transfer pathways to the oxygen atoms of the quinone. Three main topics are discussed: (1) the pathways for proton transfer involving the residues: His-H126, His-H128, Asp-L210, Asp-M17, Asp-L213, Ser-L223 and Glu-L212, which were determined by a variety of methods including the use of proton uptake inhibiting metal ions (e.g. Zn^{2+} and Cd^{2+}); (2) the rate constants for proton transfer, obtained from a 'chemical rescue' study was determined to be 2×10^5 s^{-1} and 2×10^4 s^{-1} for the proton uptake to Glu-L212 and $Q_B^{-\bullet}$, respectively; (3) structural studies of altered proton transfer pathways in revertant RCs that lack the key amino acid Asp-L213 show a series of structural changes that propagate toward L213 potentially allowing Glu-H173 to participate in the proton transfer processes.**

Key words: Buffer effect; General acid catalysis; Brönsted plot; Proton-coupled electron transfer; Hydrogen ion; Proton transport; Site-directed mutations; Bacterial photosynthesis; *Rhodobacter sphaeroides*

1. Introduction

Proton transfer reactions between proton donors and acceptors are of crucial importance for biological energy conversion in many biological systems. Many of the proton transfer reactions are coupled to other light induced or redox induced events such as electron transfer. Some examples of these proton coupled electron transfer reactions occur in the processes of oxygen evolution in photosynthesis, oxygen reduction in respiration and the quinone reduction cycle that couples electron transfer to proton pumping across biological membranes [1–3]. The determination of the X-ray crystal structure of the membrane proteins that catalyze these reactions [4–9] combined with biochemical and biophysical studies relating structure and function have provided insight into the mechanisms of this type of coupling in bioenergetic systems. Common to these systems is the requirement of a proton transfer mechanism for the uptake and/or release of protons from the interior of a protein to the exterior aqueous solution. This involves specific proton transfer pathways (often called a proton wire). In this minireview, we discuss studies of the proton coupled electron transfer reaction leading to the reduction of the quinone molecule Q_B in the bacterial reaction center (RC) from *Rhodobacter sphaeroides*. Proton coupled electron transfer in the RC has been extensively studied by many workers [10–12]. In this paper, we review more recent results that elucidate the pathway and mechanism of proton transfer.

The RC is the membrane bound pigment–protein complex that is responsible for light induced electron transfer in photosynthesis. Light initiates electron transfer from a primary electron donor D through a series of electron acceptors to a primary quinone Q_A. The reduced Q_A^- serves as the electron donor to a weakly bound quinone Q_B (Fig. 1). Following reduction of D^+ by an exogenous donor, Q_B accepts a second photo induced electron from $Q_A^{-\bullet}$, taking up two protons from solution resulting in the formation of the fully reduced dihydroquinone. The overall reaction is:

$$Q_B + 2e^- + 2H^+ + 2\,h\nu \rightarrow Q_BH_2 \qquad (1)$$

In photosynthetic membranes the reduced Q_BH_2 is released to the membrane and oxidized by the cytochrome bc_1 complex releasing the protons across the membrane into the periplasm, generating a proton gradient that drives ATP synthesis [1]. The electrons are cycled back to D^+ of the RC via a mobile electron carrier cytochrome c_2 [13]. Thus, the coupling of proton transfer and electron transfer plays an essential role in the basic process of energy transduction in photosynthesis.

2. Proton coupled electron transfer reactions

The formation of quinol occurs in two sequential light induced steps with observed rate constants $k_{AB}^{(1)}$ for the first electron reduction and $k_{AB}^{(2)}$ for the second (Eqs. 2 and 3). The first light induced reaction results in electron transfer from $Q_A^{-\bullet}$ to Q_B and is coupled to the protonation of a nearby carboxylic group Glu-L212 (Glu^- in Eq. 2).

*Corresponding author. Fax: (1)-858-822 0007.
E-mail address: mokamura@ucsd.edu (M.Y. Okamura).

Abbreviations: RC, reaction center; D, primary electron donor; Q_A and Q_B, the primary and secondary quinone electron acceptor molecules; A^-, intermediate proton acceptor group; $k_{(2)}$, apparent second order rate constant; K_D, dissociation constant of the acid; k_{ON}, k_{OFF}, the on and off rate constants for binding of the acid; k_{et}, the overall electron transfer rate constant; k_{H^+}, the overall proton transfer rate constant

0014-5793/03/$22.00
doi:10.1016/S0014-5793(03)01149-9

$$(Q_A^{-\cdot}Q_B)Glu^- + H^+ \xrightarrow{k_{H^+(1)}} (Q_A^{-\cdot}Q_B)GluH \xrightarrow{k_{et(1)}} (Q_AQ_B^{-\cdot})GluH \qquad (2)$$

where $k_{H+(1)}$ and $k_{et(1)}$ are the rate constants for proton and electron transfer, respectively [14]. The second light induced reaction resulting in electron transfer from $Q_A^{-\bullet}$ is coupled to the first direct protonation of the semiquinone. The mechanism of the proton coupled electron transfer reaction (Eq. 3) was shown to be a two step process in which fast protonation precedes the rate limiting electron transfer step [15].

$$Q_A^{-\cdot}Q_B^{-\cdot} + H^+ \xrightarrow{k_{H^+(2)}} Q_A^{-\cdot}Q_BH^{\cdot} \xrightarrow{k_{et(2)}} Q_AQ_BH^- \qquad (3)$$

where $k_{H+(2)}$ and $k_{et(2)}$ are the rate constants for proton and electron transfer, respectively. Following the finding that the RC could be co-purified with an externally bound Zn^{2+} [16], a systematic study of transition metal binding showed that Zn^{2+} and Cd^{2+} bound stoichiometrically (pH 7.8) to the RC surface and inhibited the first protonation step [17]. This resulted in a change in the rate controlling step from electron transfer ($k_{et(2)}$) to proton uptake ($k_{H+(2)}$).

Subsequent internal proton transfer of H^+ from Glu-L212 (Eq. 4) leads to the formation of quinol.

$$(Q_AQ_BH^-) - GluH \rightarrow (Q_AQ_BH_2) - Glu^- \qquad (4)$$

Note that although the H^+ in Eq. 4 is taken up from solution during the first electron transfer step (Eq. 2), it protonates Glu^- (Eq. 2) and is transferred to reduced Q_B only after the second electron transfer step (Eq. 3).

3. Pathways for proton transfer

The structure of the RC from *Rb. sphaeroides* between the surface and the catalytic $Q_B^{-\bullet}$ site is shown in Fig. 1 [18]. The two quinone molecules, Q_A and Q_B, are separated by a distance of 15 Å (edge to edge) through hydrogen bonding to the His–Fe–His metal link. The region of the protein near Q_B contains numerous acidic and polar residues that have been shown to be involved in the pathway for transfer of the two protons that are bound by the reduced quinone.

The protons involved in the reactions described by Eqs. 1–4 are taken up from the cytoplasm. Several key components of these pathways have been determined from studies of the effects of site directed mutations in isolated RCs [19–24]. Three residues (Glu-L212, Ser-L223 and Asp-L213), located near $Q_B^{-\bullet}$ (≤ 5 Å) were shown to play a crucial role. The entry point of the protons has been identified to be near His-H126, His-H128 and Asp-H124 (Fig. 1), the binding position of the proton transfer inhibitors Zn^{2+} and Cd^{2+} [25]. The importance of His-H126 and His-H128 for facilitating proton transfer into the RC was subsequently confirmed through site directed mutagenesis [24]. Located between the surface His and the internal acids are Asp-L210 and Asp-M17, which upon replacement with Asn decrease the rate of proton transfer by 100-fold [26]. The proton transfer pathways share the involvement of the surface His-H126 and His-H128 and the intermediate carboxylic acids Asp-M17, Asp-L210 and Asp-L213. At or near Asp-L213, the pathways for the two protons diverge (see Fig. 1). Transfer of H^+ to Glu-L212 (Eq. 2) occurs through intervening water molecules. Transfer directly to $Q_B^{-\bullet}$ (Eq. 3) occurs through Ser-L223. Water molecules located between the acid groups likely serve as bridges or connectors providing the missing links for hydrogen bonding chains.

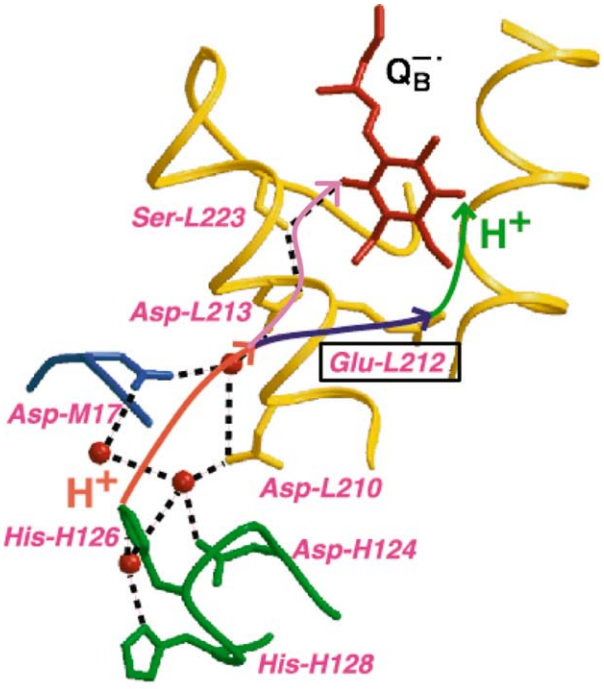

Fig. 1. Part of the RC structure showing the proton transfer pathways. Water molecules are shown as spheres [18]. Potential hydrogen bonds are indicated by dashed lines. The proton transfer pathways connecting the surface to the Q_B site share the entry point and several carboxylic acids (red line) before branching to Glu-L212 (blue line) or to $Q_B^{-\bullet}$ (magenta line). Although protonation (neutralization) of Glu-L212 is required for the first electron reduction of Q_B to proceed (Eq. 2), the proton is transferred to the proximal oxygen of reduced Q_B near His-L190 only after formation of Q_BH^- (green line). Coordinates obtained from pdb ID number 1AIJ.

The pathways for proton transfer are functionally robust and relatively insensitive to perturbations. This is shown by the observation that mutation of a single Asp residue (Asp-M17 or Asp-L210) or a single His residue (His-H126 or His-H128) near the entry point (Fig. 1) does not inhibit proton transfer sufficiently to become rate limiting. On the other hand, double mutations (Asp-M17 → Asn/Asp-L210 → Asn or His-H126 → Ala/His-H128 → Ala) inhibit the rate of proton transfer >100-fold. This suggests that at least two parallel routes are operational in the pathway regions near the proton entry points (see Fig. 1). In addition, there are other possible proton transfer routes in the interior of the protein that may include other protonatable residues (e.g. Glu-H173) and water molecules, but there is no compelling evidence that they contribute significantly to the proton transfer processes.

4. Rate constants for proton transfer

The rate constants for proton transfer reactions are fundamentally important in understanding the molecular basis of the proton transfer process. However, the proton transfer rate

constants are not directly obtained from measured rates of electron transfer since proton transfer is not the rate limiting step for either electron transfer (Eqs. 2 and 3). If, however, the rate of proton transfer is reduced sufficiently, then proton transfer becomes the rate limiting step. These situations arise when key residues in the proton transfer pathways are mutated (Fig. 1). To determine whether a change in the rate limiting step has occurred, we used the electron driving force assay [15,17], i.e. we measured the dependence of $k_{AB}^{(2)}$ on the driving force for electron transfer. When electron transfer is rate limiting, we expect from Marcus theory a ~10-fold change in rate for a 100 meV change in driving force as is observed in the native RC [15]. When the rate limiting step is proton transfer, the observed rate becomes independent of the driving force [17]. For the native RC, electron transfer is rate limiting and the measured rate provides only a lower limit for the rate constant for proton transfer. Thus, the determination of the intrinsic rate constant for proton transfer remained a challenge.

This challenge was met by using RCs with the double mutation of His-H126→Ala/His-H128→Ala. Replacement of the His with Ala resulted in an RC in which the rate limiting step in Eqs. 2 and 3 was proton uptake from solution. A detailed systematic study showed that the proton limited phase of $k_{AB}^{(1)}$ could be enhanced by addition of exogenous acids acting as proton carriers with an apparent second order rate constant $k_{(2)}$; the rate could be completely restored (chemically rescued) upon adding high concentrations of imidazole and other rescuing acids with pK_a values below 9. The active species were identified as the cationic forms of the rescuing acids based on the pH and ionic strength dependence of the rate enhancement. Values of $k_{(2)}$ were measured for rescuing acids with different pK_a values. The values of $k_{(2)}$ were at the diffusion limit of 10^{10} M^{-1} s^{-1} for low pK_a (<4) rescuers and decreased ~10-fold per pK_a unit increase above this value (Brönsted coefficient $\alpha = 1.0$) [28]. A Brönsted plot [27] of the log of the observed second order rate constant vs. pK_a (Fig. 2) was determined and interpreted in terms of the model for $k_{(2)}$ shown in Eq. 5. The change in slope of the Brönsted plot occurs at a pK_a at which the rate controlling step of $k_{(2)}$ changes. This happens when the pK_a of the donating acid approximately matches that of the acceptor group, which in our data occurs near a pK_a of 4 (Fig. 2). At this pK_a there is a change from a proton transfer limited rate (for higher pK_a acids) to a diffusion controlled rate (for lower pK_a acids). Because the final acceptor group (Glu-L212) is known to have a much different pK_a of ~8.5 [11,14,19,20], the group responsible for the change in the slope of the Brönsted plot must be an intermediate acceptor group in the proton transfer pathway. With the inclusion of this postulated intermediate proton acceptor group that we shall call A, the chemical rescue is composed of four steps (Eq. 5): (1) the binding of the rescuing acid, RH^+; (2) proton transfer to an intermediate proton acceptor group, A^-; (3) proton transfer to the final proton acceptor group, Glu^-; Glu-L212 and (4) dissociation of the neutral rescuing acid, R.

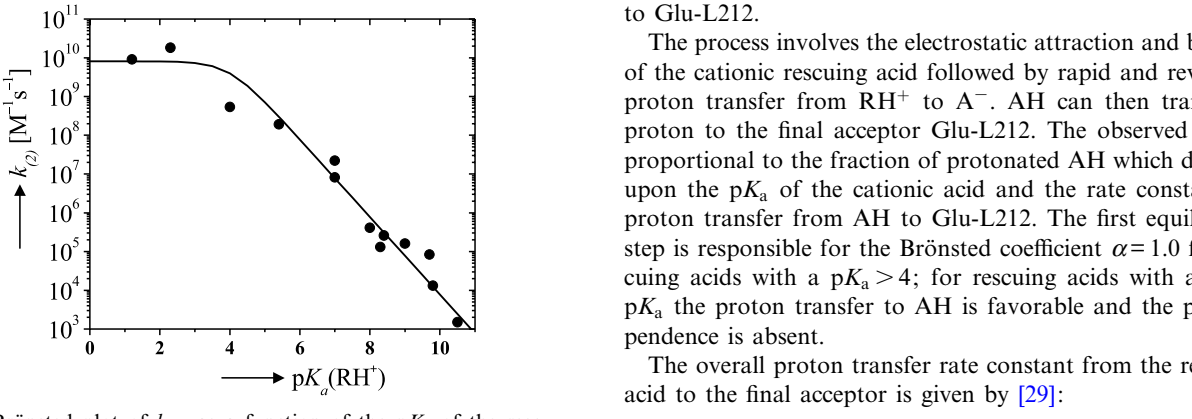

Fig. 2. Brönsted plot of $k_{(2)}$ as a function of the pK_a of the rescuing acid in the HA(H126)/HA(H128) mutant RC (modified from [28]). Below p$K_a \approx 4$, $k_{(2)}$ reaches the diffusion limit of ~10^{10} M^{-1} s^{-1}. At higher pK_a values, $k_{(2)}$ decreases with increasing pK_a, characteristic of general acid catalysis. The slope of $k_{(2)}$ versus pK_a changes when the pK_a of the bound donating acid matches that of the acceptor. Since the pK_a of the final acceptor Glu-L212 is much larger (p$K_a \approx 8.5$) than the pK_a at the break of the Brönsted plot, there must exist an intermediate acceptor group (A^-) within the proton transfer pathway. The data were fitted (solid curve) using Eq. 5. Note the good quality of the fit over the range of ~9 pK_a units (see [28] for details).

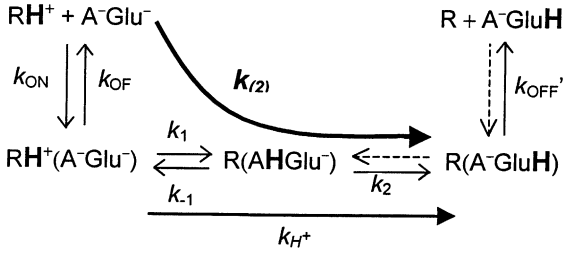

(5)

where RH^+ and R are the protonated and unprotonated forms of the rescuing acid, respectively; A^- is the intermediate proton acceptor group; Glu is the final proton acceptor Glu-L212 (Eq. 2); k_{ON} and k_{OFF} are the on and off rate constants of the acid molecule; k_{OFF}' is the off rate of the unprotonated acid molecule; k_1 and k_{-1} are the forward and reverse proton transfer rate constants from the acid to A^-; and k_2 is the forward proton transfer rate constant from AH to Glu-L212.

The process involves the electrostatic attraction and binding of the cationic rescuing acid followed by rapid and reversible proton transfer from RH^+ to A^-. AH can then transfer a proton to the final acceptor Glu-L212. The observed rate is proportional to the fraction of protonated AH which depends upon the pK_a of the cationic acid and the rate constant for proton transfer from AH to Glu-L212. The first equilibrium step is responsible for the Brönsted coefficient $\alpha = 1.0$ for rescuing acids with a p$K_a > 4$; for rescuing acids with a lower pK_a the proton transfer to AH is favorable and the pK_a dependence is absent.

The overall proton transfer rate constant from the rescuing acid to the final acceptor is given by [29]:

$$k_{(2)} = k_{ON}\frac{k_{H^+}}{k_{OFF} + k_{H^+}} \quad (6)$$

where k_{H^+} is the proton transfer rate from the rescuing acid to Glu-L212. For the case of imidazole, this simplifies to the expression $k_{(2)} = k_{H^+}/K_D$, where K_D is the dissociation constant [28]. A value of $K_D = 10$ mM was found for trimethyl ammonium, and assumed to be the same for all cationic acids given the good linear dependence of log $k_{(2)}$ on pK_a (Fig. 2).

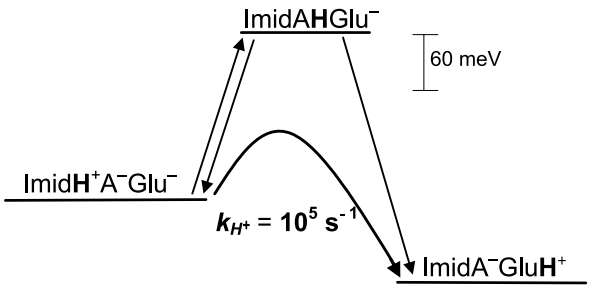

Fig. 3. Energy level diagram of the states involved in the proton transfer reactions from the bound imidazole ($ImidH^+$) to the final proton acceptor Glu-L212 (modified from [28]). Proton transfer proceeds through an intermediate state AH which is higher in energy than the initial state by $\delta\Delta G_1 \approx 240$ meV. Proton transfer can then proceed downhill by $\sim$330 meV to Glu-L212. The resultant forward proton transfer rate $k_{H^+} \cong 2\times10^5$ s^{-1} is indicated.

Since the rescue of double mutant RC with imidazole was indistinguishable from the native RC and the functional group of imidazole is the same as the native His, we used the bound imidazolium as the model for the native His. From the value of $k_{(2)}$ imidazole $= 2\times10^7$ M^{-1} s^{-1}, the value of $k_{H^+} = 2\times10^5$ s^{-1} is obtained for proton transfer from the bound imidazole group to Glu-L212. Similar measurements of chemical rescue of $k_{AB}^{(2)}$ gave a value of $k_{H^+} = 2\times10^4$ s^{-1} for the proton transfer from the bound imidazole group to $Q_B^{-\bullet}$. The reason for this smaller value is mostly due to the smaller pK_a of $Q_B^{-\bullet}$ compared to that of Glu-L212.

The relative energy levels for proton transfer from the surface bound acid to Glu-L212 is shown in Fig. 3. This energy landscape is determined by the free energies of protonation for the individual groups. The pK_a of Glu-L212 in the double His mutant RC was determined from the pH titration of the slower proton-limited phase of $k_{AB}^{(1)}$. This gave a value of 8.5 for pK_a(Glu-L212) [24]. The pK_a of the intermediate acceptor group is given approximately by the pK_a at which the Brönsted plot changes slope, which occurs at $\sim$4. (There is a slight correction of $\sim$1 unit to this value, discussed in [28].) The pK_a of 6.8 of the surface His was obtained from a study of the pH dependence of Cd^{2+} binding to the native RC [30], a technique that had been applied to other systems [31,32]. Thus, we can summarize the transfer in two steps. The first step is the fast reversible proton transfer from the bound protonated imidazole to A^-, which is unfavorable by $\sim$240 meV. This is followed by an $\sim$330 meV favorable proton transfer from AH to Glu-L212 (Fig. 3).

These proton transfer rates are roughly the same as those observed in the extensively studied carbonic anhydrase (CA) enzyme [33,34] even though proton transfer in the RC occurs over a longer distance of $\sim$20 Å compared to $\sim$10 Å for CA. The fast rate over the longer distance is due to the intermediate state(s) which breaks the reaction into two (or more) shorter proton transfer steps. In this work, we assume, for

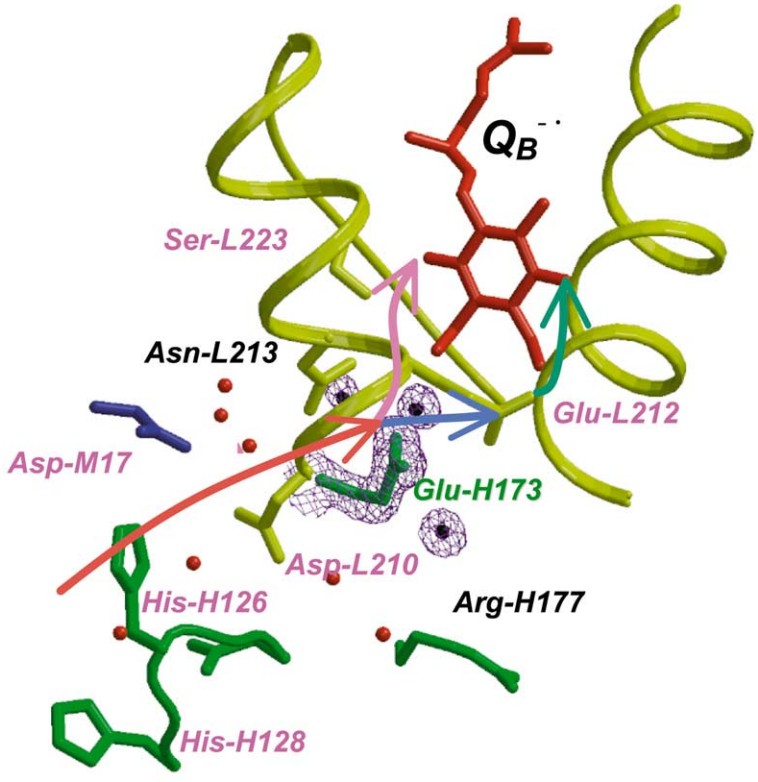

Fig. 4. Potential proton transfer pathways in the Asp-L213→Asn/Arg-M233→Cys revertant RC structure [39]. The site of the parental mutation (Asn-L213) and a resultant structural change of Arg-H177 are labeled in black. The potential proton transfer pathway leading to $Q_B^{-\bullet}$ is shown in red and magenta, the branch leading to Glu-L212 in blue. $Q_B^{-\bullet}$ was placed at the location found in the native RC. The structure of the neutral Q_B state was determined and was found to be at the same location as that for Q_B in the native RC. Key amino acid residues are shown (labeled in magenta). Shown is the electron density (in blue at 1.5 σ) for the new position of Glu-H173 (labeled in green) and three water molecules, proposed to be the functionally important changes. These water molecules, located nearby at positions not observed in the native structure, could provide bridges to and from Glu-H173 in the revertant structure. Other pathways, including one through L210 and its nearby water molecules, are longer but still possible (not shown).

simplicity, only one intermediate state A, although other, as yet unresolved states, may exist.

5. Proton transfer in revertant RCs lacking Asp-L213

A key amino acid in the native RC of *Rb. sphaeroides* is Asp-L213 [19–21]. Its replacement with Asn [DN(L213)] decreases the proton transfer rates $\sim 10^6$-fold (pH 7.5) resulting in a photosynthetically incompetent RC [35]. It was shown that substitution of Asn-M44 by Asp suppressed this effect [36,37]. Being structurally close to Ser-L223, it was proposed that Asp-M44 could substitute for the missing carboxylate at L213. This also provided an explanation for the lack of sequence conservation of Asp-L213 in different photosynthetic bacterial species. Several species (e.g. *Blastochloris viridis*) have Asn at the homologous location of L213 and Asp at the homologous location of M44 [36,37]. However, additional photosynthetic revertants obtained by several groups [35,38] revealed second site suppressor mutations that do not re-introduce a carboxylic acid, e.g. Arg-M233→Cys or Arg-H177→His. In these two cases, the rates of proton transfer have been increased $>10^4$-fold from that of DN(L213).

To understand the structural basis of the increase in proton transfer, the crystal structures of the mutants were determined [39]. We will focus on some details of the structure of the revertant with the M233 suppressor mutation which was obtained to a resolution of 1.8 Å. Several observations suggest that the suppressor mutation itself is not likely to be directly involved in the new proton transfer pathway that circumvents the Asn-L213. First, the mutation results in the replacement of Arg with Cys, which is not a proton transfer component. Second, the site of the suppressor mutation is located >10 Å from the parental L213 mutation and the Q_B catalytic site. However, the M233 mutation results in structural rearrangements of Glu-H173 and the incorporation of new water molecules near L213 and the Q_B region (Fig. 4). The changes to Glu-H173 are also found in the structure of the H177 revertant even though the structure near M233 differs. Thus, we propose that the reorientation of Glu-H173 and incorporation of the new water molecules near L213 are the functionally relevant changes.

The entry point for proton uptake was identified to be at or near the same location as in the native RC by the similar inhibitory effect of binding of Cd^{2+} [40]. Since the structure shows this region to be the same in the revertant and native RCs, the Cd^{2+} should bind to this region in the revertant RCs. Additional support for the binding location of the Cd^{2+} comes from the similar pH dependence of K_D which shows the involvement of titrable ligands that have essentially the same pK_a values as His-H126 and His-H128 in the native RC. Thus, the entry point for proton transfer is located near His-H126 and His-H128. Given the defined starting points near His-H126 and His-H128 and ending points at Glu-L212 and $Q_B^{-\bullet}$, potential proton transfer pathways could be identified. The most likely pathways are similar to those found in the native RC with Glu-H173 being a likely replacement for the missing Asp at L213. Important for the involvement of Glu-H173 are three water molecules that provide connectivity between Glu-H173 and the oxygen atoms of $Q_B^{-\bullet}$ and Asp-L210 which is connected to the proton entry point. Thus, although neither suppressor mutation re-introduces a carboxylic acid, the resultant structural rearrangements allow an alternative acid, Glu-H173, to become part of the new proton transfer pathway.

Studies of revertant systems like these provide a means of identifying crucial features for fast proton transfer. Of primary importance in the RC system is the identification of the altered proton transfer pathway and the concomitant delineation of the importance of Glu-H173 in proton transfer. Another important aspect is the relation between the proton transfer rate constant (i.e. the effectiveness) and the details of the altered proton transfer pathways. Given the altered proton transfer pathways, the rates are not likely to be the same. It would be important to determine the rate constants to relate to the revertant structures.

Acknowledgements: We thank Herbert Axelrod, Qiang Xu, Charlene Chang, Edward Abresch, Ali Tehrani and J. Thomas Beatty (UBC, Canada) for helpful discussions and technical assistance. This work was supported by the National Science Foundation (NSF MCB99-82186) and the National Institutes of Health (NIH GM 41637 and NIH GM 13191).

References

[1] Cramer, W.A. and Knaff, D.B. (1990) Energy Transduction in Biological Membranes, Springer-Verlag, New York.
[2] Brzezinski, P. and Ådelroth, P. (1998) J. Bioenerg. Biomembr. 30, 99–107.
[3] Tommos, C. and Babcock, G.T. (2000) Biochim. Biophys. Acta 1458, 199–219.
[4] Deisenhofer, J., Epp, O., Miki, K., Huber, R. and Michel, H. (1984) J. Mol. Biol. 180, 385–398.
[5] Allen, J.P., Feher, G., Yeates, T.O., Komiya, H. and Rees, D.C. (1987) Proc. Natl. Acad. Sci. USA 84, 5730–5734.
[6] Tsukihara, T., Aoyama, H., Yamashita, E., Tomizaki, T., Yamaguchi, H., Shinzawaitoh, K., Nakashima, R., Yaono, R. and Yoshikawa, S. (1996) Science 272, 1136–1144.
[7] Iwata, S., Ostermeier, C., Ludwig, B. and Michel, H. (1995) Nature 376, 660–669.
[8] Xia, D., Yu, C.-A., Kim, H., Xian, J.-Z., Kachurin, A.M., Zhang, L., Yu, L. and Deisenhofer, J. (1997) Science 277, 60–66.
[9] Berry, E., Guergova-Kuras, M., Huang, L. and Crofts, A. (2000) Annu. Rev. Biochem. 69, 1005–1075.
[10] Shinkarev, V. and Wraight, C. (1993) in: The Photosynthetic Reaction Center (Deisenhofer, J. and Norris, J., Eds.), pp. 193–255, Academic Press, San Diego, CA.
[11] Sebban, P., Maróti, P. and Hanson, D. (1995) Biochimie 77, 677–694.
[12] Okamura, M., Paddock, M., Graige, M. and Feher, G. (2000) Biochim. Biophys. Acta 1458, 148–163.
[13] Blankenship, R.E., Madigan, M.T. and Bauer, C.E. (1995) Anoxygenic Photosynthetic Bacteria, Kluwer Academic, Dordrecht.
[14] Ådelroth, P., Paddock, M.L., Sagle, L.B., Feher, G. and Okamura, M.Y. (2000) Proc. Natl. Acad. Sci. USA 97, 13086–13091.
[15] Graige, M.S., Paddock, M.L., Bruce, J.M., Feher, G. and Okamura, M.Y. (1996) J. Am. Chem. Soc. 118, 9005–9016.
[16] Utschig, L.M., Ohigashi, Y., Thurnauer, M.C. and Tiede, D.M. (1998) Biochemistry 37, 8278–8281.
[17] Paddock, M.L., Graige, M.S., Feher, G. and Okamura, M.Y. (1999) Proc. Natl. Acad. Sci. USA 96, 6183–6188.
[18] Stowell, M.H., McPhillips, T.M., Rees, D.C., Soltis, S.M., Abresch, E. and Feher, G. (1997) Science 276, 812–816.
[19] Paddock, M.L., Rongey, S.H., Feher, G. and Okamura, M.Y. (1989) Proc. Natl. Acad. Sci. USA 86, 6602–6606.
[20] Takahashi, E. and Wraight, C.A. (1990) Biochim. Biophys. Acta 1020, 107–112.
[21] Takahashi, E. and Wraight, C.A. (1992) Biochemistry 31, 855–866.
[22] Sebban, P., Maróti, P., Schiffer, M. and Hanson, D.K. (1995) Biochemistry 34, 8390–8397.
[23] Alexov, E.G. and Gunner, M.R. (1999) Biochemistry 38, 8253–8270.

[24] Ådelroth, P., Paddock, M.L., Tehrani, A., Beatty, J.T., Feher, G. and Okamura, M.Y. (2001) Biochemistry 40, 14538–14546.
[25] Axelrod, H.L., Abresch, E.C., Paddock, M.L., Okamura, M.Y. and Feher, G. (2000) Proc. Natl. Acad. Sci. USA 97, 1542–1547.
[26] Paddock, M.L., Ådelroth, P., Chang, C., Abresch, E.C., Feher, G. and Okamura, M.Y. (2001) Biochemistry 40, 6893–6902.
[27] Brönsted, J.N. and Pedersen, K. (1923) Z. Phys. Chem. A 108, 185.
[28] Paddock, M.L., Ådelroth, P., Feher, G., Okamura, M.Y. and Beatty, J.T. (2002) Biochemistry 41, 14716–14725.
[29] Fersht, A. (1999) Structure and Mechanism in Protein Science: A Guide to Enzyme Catalysis and Protein Folding, W.H. Freeman, New York.
[30] Paddock, M.L., Sagle, L., Tehrani, A., Beatty, J.T., Feher, G. and Okamura, M.Y. (2003) Biochemistry 42, 9626–9632.
[31] Link, T.A. and von Jagow, G. (1995) J. Biol. Chem. 270, 25001–25006.
[32] Cherny, V.V. and DeCoursey, T.E. (1999) J. Gen. Physiol. 114, 819–838.
[33] Earnhardt, J.N., Tu, C. and Silverman, D.N. (1999) Can. J. Chem. 77, 726–732.
[34] Silverman, D.N. (2000) Biochim. Biophys. Acta 1458, 88–103.
[35] Paddock, M.L., Senft, M.E., Graige, M.S., Rongey, S.H., Turanchik, T., Feher, G. and Okamura, M.Y. (1998) Photosynth. Res. 55, 281–291.
[36] Hanson, D.K., Nance, S.L. and Schiffer, M. (1992) Photosynth. Res. 32, 147–153.
[37] Rongey, S.H., Paddock, M.L., Feher, G. and Okamura, M.Y. (1993) Proc. Natl. Acad. Sci. USA 90, 1325–1329.
[38] Hanson, D.K., Baciou, L., Tiede, D.M., Nance, S.L., Schiffer, M. and Sebban, P. (1992) Biochim. Biophys. Acta 1102, 260–265.
[39] Xu, Q., Abresch, E.C., Axelrod, H.L., Paddock, M.L., Okamura, M.Y. and Feher, G. (2003) Biophys. J. 84, 273a.
[40] Paddock, M.L., Xu, Q., Feher, G. and Okamura, M.Y. (2003) Biophys. J. 84, 274a.